

This item was submitted to [Loughborough's Research Repository](#) by the author.
Items in Figshare are protected by copyright, with all rights reserved, unless otherwise indicated.

EuroTracker (R) dyes: design, synthesis, structure and photophysical properties of very bright europium complexes and their use in bioassays and cellular optical imaging

PLEASE CITE THE PUBLISHED VERSION

<http://dx.doi.org/10.1039/c4dt02785j>

PUBLISHER

© The Royal Society of Chemistry

VERSION

NA (Not Applicable or Unknown)

PUBLISHER STATEMENT

This work is made available according to the conditions of the Creative Commons Attribution-NonCommercial-NoDerivatives 4.0 International (CC BY-NC-ND 4.0) licence. Full details of this licence are available at: <https://creativecommons.org/licenses/by-nc-nd/4.0/>

LICENCE

CC BY-NC-ND 4.0

REPOSITORY RECORD

Butler, Stephen J., Martina Delbianco, Laurent Lamarque, Brian K. McMahon, Emily R. Neil, Robert Pal, David Parker, James W. Walton, and Jurriaan M. Zwieter. 2019. "Eurotracker (R) Dyes: Design, Synthesis, Structure and Photophysical Properties of Very Bright Europium Complexes and Their Use in Bioassays and Cellular Optical Imaging". figshare. <https://hdl.handle.net/2134/18759>.

EuroTracker Dyes: design, synthesis, structure and photophysical properties of very bright europium complexes and their use in bioassays and cellular optical imaging

Stephen J Butler^a, Martina Delbianco^a, Laurent Lamarque^b, Brian K McMahon^a, Emily R Neil^a, Robert Pal^a, David Parker ^{*a}, James W Walton^a and Jurriaan M. Zwier^b

^a Department of Chemistry, Durham University, South Road, Durham DH1 3LE, UK

^b CisBio Bioassays, Parc Marcel Boiteux, BP 84175, 30200 Codolet, France

email: david.parker@dur.ac.uk

Dedicated to the memory of Professor Ken Wade FRS (1932 - 2014)

Introduction

In 1852, George Stokes introduced the word fluorescence to describe the phenomenon of ‘internal reflection’ – an emission of blue light - that he had observed when examining sunlit samples of the mineral fluor spar, and that Herschel, Brewster and Becquerel had described earlier when irradiating solutions of quinine salts. ¹ The calcium fluorite samples Stokes examined were doped with Eu(II), and led to a blue emission; with an Yb(II) dopant, yellow-green light is emitted. ² These beautiful mineral samples are still being mined in upper Weardale, County Durham in the North-East of England, and create a local link to the series of very bright, red-emitting Eu(III) complexes that are described herein.

Europium emission occurs on a millisecond timescale over the range 580 to 720 nm, and has been used for many years in a wide range of applications in the materials and biosciences, ³⁻⁷ from security printing in bank notes to reporters for time resolved bioassays. As the transitions between f electronic energy levels are symmetry forbidden, direct excitation of the Eu ion is very inefficient, and the ⁵D₀ Eu excited state is preferably populated via a sensitisation mechanism. This process involves light absorption by a proximate chromophore, followed by intramolecular energy transfer to the Eu ion. In order that the Eu ion emits light with a high overall quantum yield in water, it needs to be efficiently shielded from the external environment, to minimize non-radiative deactivation processes, such as electron transfer or vibrational energy transfer to overtones of XH oscillators (X = O, N and C). ⁸ Thus, the ligand used to complex the Eu ion must be octa- or nonadentate to exclude coordinated water molecules and should encapsulate the metal ion effectively. The brightness, *B*, of the complex is the key parameter to maximize in this context. It is the product of the molar extinction coefficient, ϵ , at λ_{exc} and the overall quantum yield for Eu emission, ϕ_{em} , in

the background medium used. For excitation at 337 or 355 nm in aqueous solutions, typical values of B for Eu complexes lie in the range 1 to 3 $\text{mM}^{-1}\text{cm}^{-1}$ ^{3,5,9,10} compared to the value of 9 $\text{mM}^{-1}\text{cm}^{-1}$ reported for the terbium cryptate, Tb-LumiphorTM, that is used as a donor in a variety of FRET assays. ¹¹

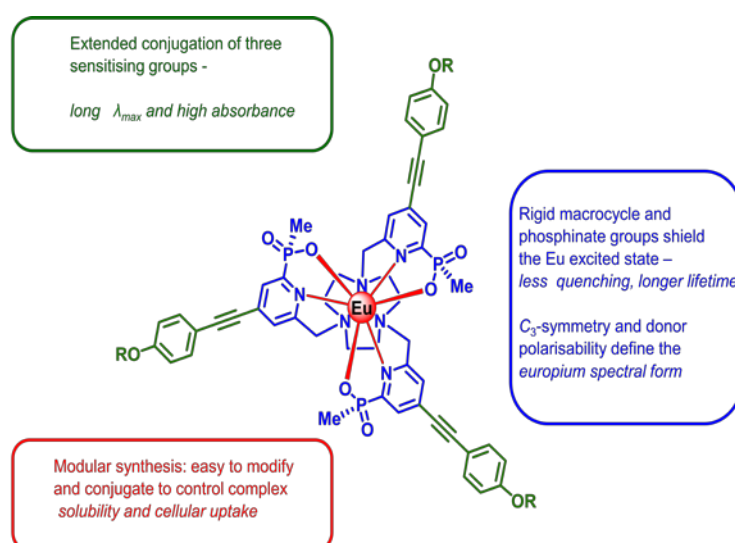
The long-lived nature of Eu emission allows its selective detection in time-resolved measurements, avoiding the experimental complications that may occur from light scattering or interference from endogenous fluorescence. For applications in optical imaging using luminescence microscopy, probe brightness needs to be assessed with due consideration to the time-resolved measurement and the local concentration of the probe, by using the following expanded relationship for probe brightness, B' , eq. 1: ¹²

$$B'(\lambda, c) = \eta \varepsilon \phi \int e^{-kt} . dt \quad (1)$$

When applied to cellular imaging, c is the complex loading concentration, λ is the excitation wavelength, k is the radiative rate constant for emission and η is an accumulation parameter, reflecting the amount of complex internalised. The integral has limits $(t_{\text{acq}} + t_{\text{d}})$ and t_{d} ; t_{acq} is the spectroscopic integration time or microscopy acquisition time and t_{d} is the delay time following pulsed excitation.

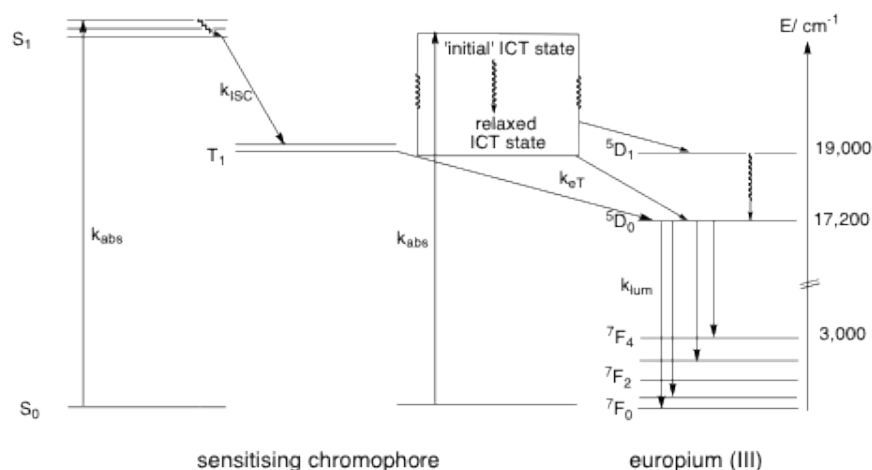
Design criteria for very bright europium complexes

Given that Eu(III) most commonly adopts a coordination number of nine, nonadentate ligands have been often considered and can be based on various C_3 symmetric core structures, such as acyclic triamines or triaza-macrocycles, such as triazacyclononane (9-N₃). The 9-N₃ macrocyclic ring is



Scheme 1 The essential design elements and structural features in emissive Eu probe design.

conformationally rigid and its chelate bite is matched to the requirements of small octahedral ions (e.g. Fe(III), Ga(III), Ni(II), Co(III))^{13,14} as well as larger lanthanide ions capable of adopting a tri-capped trigonal prismatic coordination geometry.¹⁵ The primary binding free energy term in Eu(III) coordination complexes is Coulombic. The tripositive ion therefore requires a trianionic ligand to enhance complex stability, and carboxylates, phosphinates and phenolates can be considered as preferred donors. The latter two series afford a greater steric demand around the Eu ion, and variation of the substituent at P or on the phenolate ring gives control to the extent of shielding of the excited Eu ion, (Scheme 1), inhibiting collisional deactivation processes. The spectral form of Eu emission is a sensitive function of local complex symmetry and donor atom polarisability (*vide infra*).^{3,16-18} The imposition of local C₃ symmetry coupled with the introduction of more polarisable ligand donors (e.g. py-N > amine-N > O; carboxylate O > phosphinate O) leads to enhanced emission intensity of the electric-dipole allowed transitions around 610-620 nm (⁵D₀ to ⁷F₂) and to lower relative intensity in the other emission bands.



Scheme 2 Jablonski diagram illustrating sensitised emission of Eu(III), either via an intermediate chromophore triplet or a solvent-relaxed internal charge transfer excited state.

In sensitized emission, the structure of the chromophore requires careful consideration in order to define the excitation wavelength, maximize absorbance at this wavelength and facilitate intramolecular energy transfer to populate the Eu(III) excited state. Given that common lasers operate at 337 and 355 nm, powerful laser-driven white light sources operate to 380 nm and cheap LEDs function at 385 and 365 nm, these are the preferred target wavelengths. Until recently, most chromophores were designed based on the premise that the mechanism of Eu excitation involved a triplet excited state, with an energy of >19,000 cm⁻¹ (Eu ⁵D₀ and ⁵D₁ excited states lie at 17,200 and 19,000 cm⁻¹, Scheme 2), a small singlet-triplet energy gap to favour intersystem crossing and a relatively high chromophore oxidation potential, to minimize charge transfer quenching of the singlet excited state by the proximate

Eu(III) ion.^{3,9,19} Following the definition of pyridyl-alkynyl-aryl chromophores (Scheme 1) with an intense internal charge transfer (ICT) transition, tunable by substitution of the aromatic groups, an expanded series of chromophores has emerged, each with an extinction coefficient of about $20 \text{ mM}^{-1} \text{ cm}^{-1}$ ^{20,21} (Scheme 2). Energy transfer to a Eu ion, coordinated by one or more of the pyridyl N atoms is very efficient, and the 9-N₃-based tris-pyridyl-alkynyl-aryl Eu complexes possess a brightness of around $15 \text{ to } 30 \text{ mM}^{-1} \text{ cm}^{-1}$ in water or methanol following excitation in the range 337 to 360 nm. Such a value for the probe brightness is higher than that of red fluorescent protein ($17 \text{ mM}^{-1} \text{ cm}^{-1}$).^{7,21,22}

The ease of ligand synthesis and of structural permutation is an important final aspect in probe design, (Scheme 1). For example, the ability to tune complex hydrophilicity and to enable linkage to targeting groups or to permit bio-conjugation are essential requirements in devising a family of complexes. The more obvious linkage points to the core structure, described above, are on the 9-N₃ ring carbon, thereby introducing a stereogenic centre, or on the peripheral aryl groups, such as via the alkoxy substituents. In the latter case, desymmetrisation of the complex requires that one of the alkynyl moieties be distinguished from the other two. In this regard, the intermediacy of mono-BOC-9-N₃ permits selective dialkylation and allows differentiation of the third chromophore group.²³

Structural Analysis of Europium Complexes in C₃ Symmetry

The structures of the parent Eu complexes, [Eu.L¹⁻³], have been determined by X-ray crystallography, (Figure 1); in each case an isostructural series was defined across the whole 4f block series.²⁴⁻²⁷

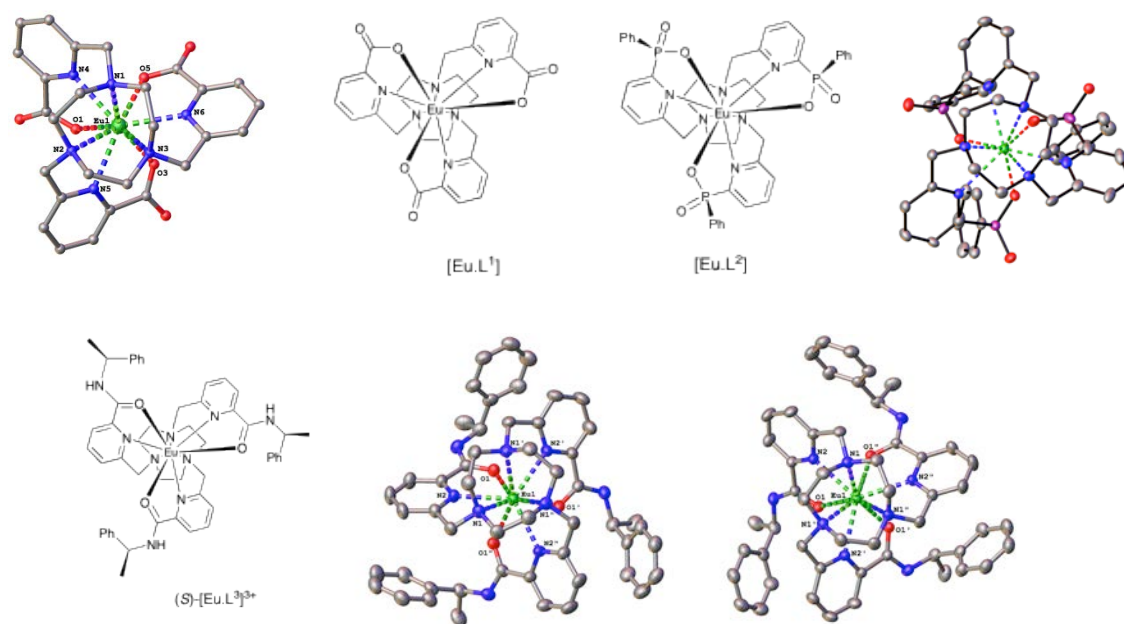


Figure 1 Views from below, into the 9-N₃ ring for the C₃ symmetric X-ray structures of *Upper left*: Λ -[Eu.L¹]; *upper right*: Λ -[Eu.L²] (i.e the R - Λ - $\delta\delta\delta$ isomer); *lower S- Λ -($\lambda\lambda\lambda$)-[EuL³]³⁺* (left) and *R- Λ -($\delta\delta\delta$)-[EuL³]³⁺* (right) (120 K) (CCDC numbers: 206375-8; 836097-102; 965909-11)²⁴⁻²⁷

In these structures, the europium ion adopts a tricapped trigonal prismatic geometry, and the complex exists as a Δ/Λ racemate in solution. Resolution of the triphosphinate and tricarboxylate complexes by chiral HPLC has been achieved²⁸, and the half-lives for racemisation at 333K in water were 185(\pm 20) and 245(\pm 35) hours respectively, compared to 5 milliseconds for the tris-chelate complex $[\text{Eu}(\text{DPA})_3]^{3-}$ measured under the same conditions, where dissociative ligand exchange provides a much faster pathway for racemisation.

The introduction of an *S* chiral substituent on the amide moiety in $[\text{Eu.L}^3]^{3+}$ induced preferential formation of the Δ complex, with an isomer ratio of 7:1 (Δ/Λ) being observed in solution by ^1H NMR. Complete stereocontrol, leading to preferential formation of one enantiomer, was observed following introduction of a chiral centre directly onto the 9- N_3 ring. Thus, a C-alkyl (alkyl = Me, ^iPr or benzyl) 9- N_3 platform derived from an *R* amino-acid precursor²⁹ led to formation of the Δ complex only, confirmed by NMR and HPLC analyses.²⁸

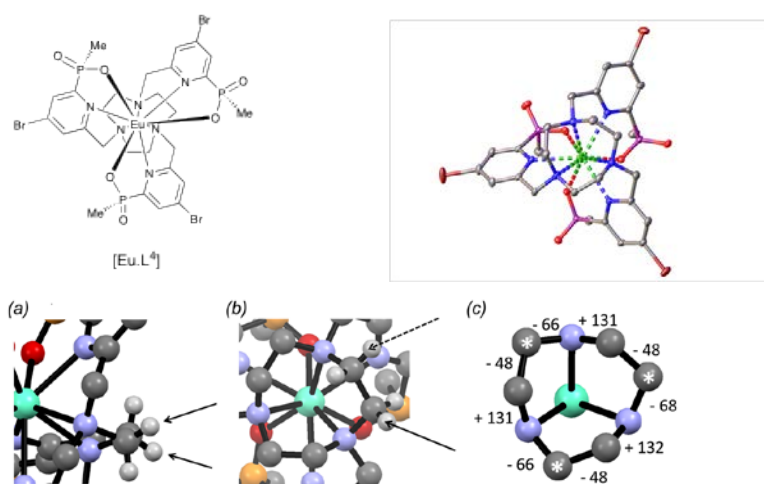


Figure 2 *upper*: Crystal structure of *SSS-Δ*-($\lambda\lambda\lambda$) $[\text{Eu.L}^4]$ (CCDC 948247)²⁸; *lower*: (a) the pseudo-equatorial positions of the pro-*R* hydrogens on the ring; (b) the corner position of the pro-*R* hydrogen (filled arrow where a C-substituent will prefer to reside), vs the side position of the pro-*R* hydrogen (dashed arrow); (c) the ring torsional angles - 'corner' carbons are marked with * (i.e. those sites between two gauche bonds, thereby defining the rigid quadrangular [333] ring conformation).

The very high stereoselectivity (>97%) observed in complex formation for the ring C-substituted series of triazacyclononane complexes was rationalised by considering the X-ray structure of the *para*-bromo derivative, $[\text{Eu.L}^4]$. The enantiomer shown (Fig. 2) has an *S* configuration at phosphorus and the complex helicity is Δ (or *P*). The Δ configuration was shown by CPL and CD studies to be formed in complexes with an *R*-stereogenic centre at the ring carbon. In this case, the pro-*R* hydrogen atom, which is the site where the ring substituent would reside, is in one of two pseudo-equatorial positions (Fig. 2a). To minimize steric repulsion, the most likely site occupied by the C-substituent is that directed away from

the three pyridyl arms (Fig. 2b), consistent with substitution of a corner (rather than a side) carbon atom (Fig. 2c).

The structure of the *p*-methoxyphenyl-alkynyl-pyridyl complex, [Eu.L⁵] has been reported.²³ In this case the complex was slightly distorted from C₃ symmetry, and the phosphorus phenyl substituents were directed away from the plane of the 9-N₃ ring to create a significant steric barrier (Figure 3). In agreement with this observation, the emission lifetime of the Eu(III) ion in [Eu.L⁵] was 30% longer compared to the carboxylate analogue in water,²¹ consistent with reduced local quenching by closely diffusing waters and an increased complex rigidity.

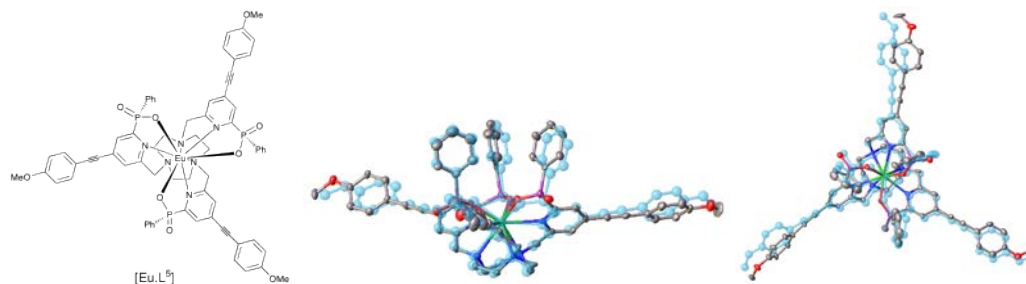
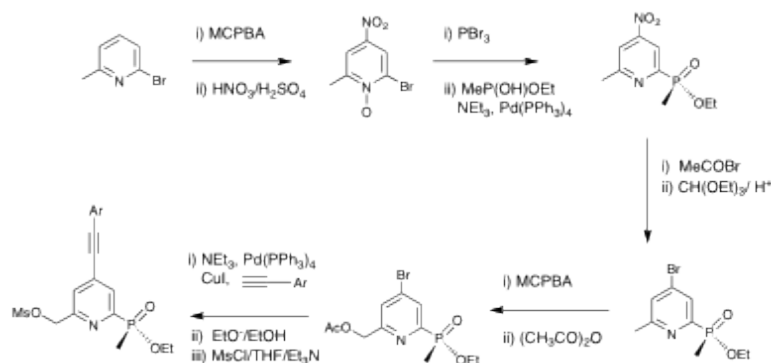


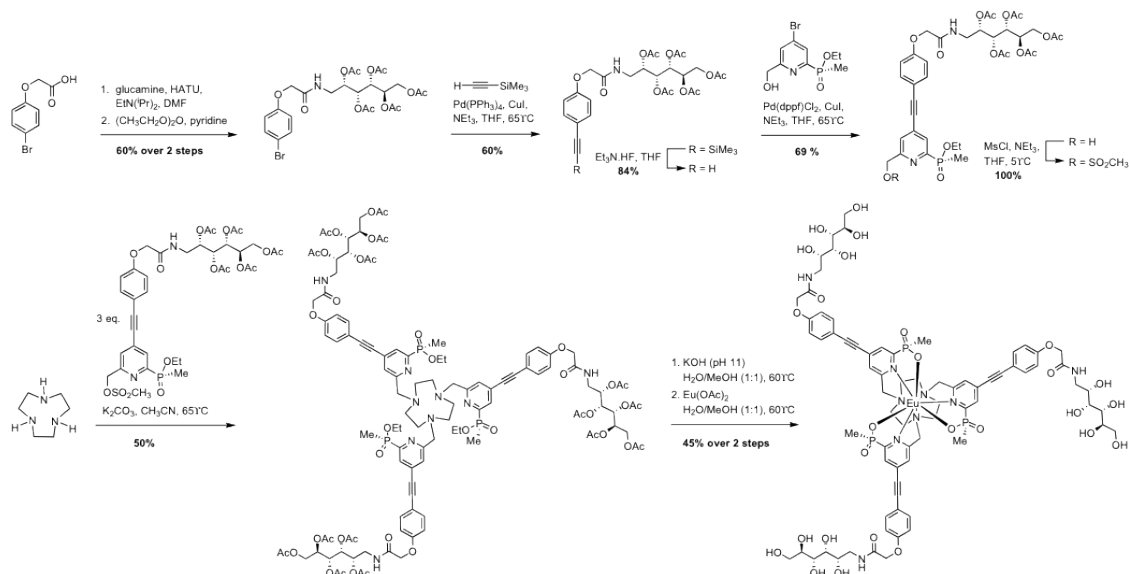
Figure 3 Experimental X-ray (*bold*) and DFT calculated (*ghost*: Y analogue) structures for the *p*-methoxyphenyl-alkyne derivative, [Eu.L⁵], highlighting the steric bulk afforded by the three P-phenyl substituents that shield the upper face of the complex (CCDC 857545).^{21,23}

Synthesis of the chromophores and complexes

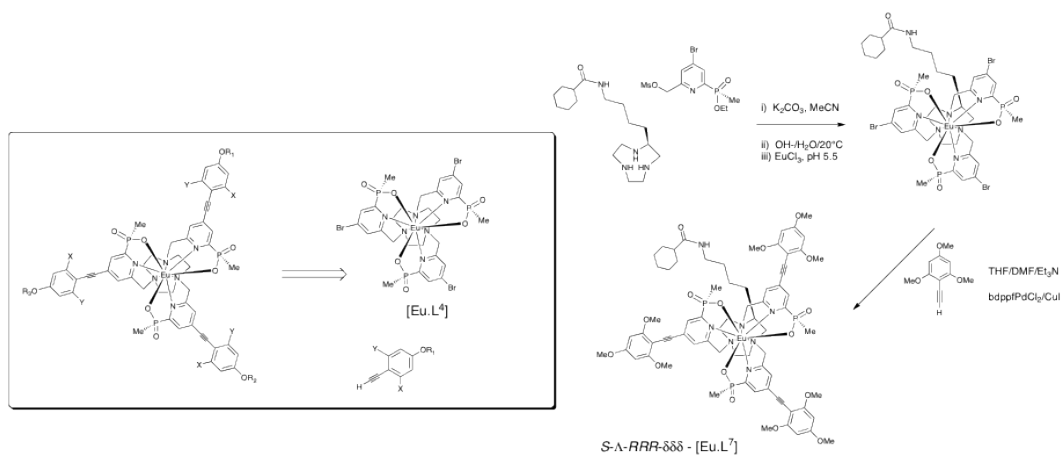
A simple retrosynthetic analysis of the target Eu complexes, such as [Eu.L⁵], reveals that the key reactions involve creation of a C-C bond between a 4-substituted pyridine and an aryl substituted alkyne, and a C-N bond-forming reaction between the ring N and a suitable alpha-substituted pyridylmethyl electrophile. A representative synthesis of a 2,4,6-trisubstituted pyridine (Scheme 3) highlights the early introduction of the C-P bond, via palladium catalysed insertion into a P-H bond, followed by intramolecular CH activation of the ring methyl group, via a Boekelheide rearrangement of the pyridine N-oxide. A Sonogashira coupling reaction generates the conjugated alkyne, and subsequent mesylation of the unmasked alcohol provides the required electrophile to alkylate the 9-N₃ ring.^{12,21,23}



Scheme 3 Synthesis of a typical 2,4,6-trisubstituted pyridine intermediate.^{12,21,23}

Scheme 4 Synthesis of the tris-glucamide derivative, [Eu.L⁶].^{12,30}

The linear forward synthesis of a complex functionalized at the phenylalkoxy position (Scheme 4) is typical of more than a dozen examples in which the Eu(III) ion is introduced in the final step, and the neutral complex is readily purified by reverse phase HPLC. An alternative, more divergent, strategy has been implemented wherein the 4-bromopyridyl europium complex, [Eu.L⁴] is used as a common intermediate (Scheme 5). This strategy allows the synthesis of a wide range of complexes with different aryl-alkynyl moieties, using the Sonogashira reaction in a product-forming step.³¹

Scheme 5 Retrosynthetic analysis and an example of the synthesis of an *S*-lysine derived enantiopure complex, Λ -[Eu.L⁷].³¹

Photophysical properties of europium complexes

The emission spectral form of the parent complexes, [Eu.L¹⁻³], strongly resembles that of [Eu(DPA)₃]³⁺, with a ratio of intensities of the $\Delta J = 2/\Delta J = 1$ bands (around 616 and 590 nm: Scheme 2) of between 4 and 5 to one in each case. In contrast, for the C₃-symmetric

complexes $[\text{Eu}(\text{ODA})_3]^{3-}$ and $[\text{Eu}(\text{IDA})_3]^{3-}$ (ODA = oxydiacetate; IDA = iminodiacetate; DPA = 2,6-pyridine-dicarboxylate),³² in which the same number of transitions is observed, the $\Delta J = 2/\Delta J = 1$ intensity ratio is near unity for $[\text{Eu}(\text{ODA})_3]^{3-}$ and 2.5:1 for $[\text{Eu}(\text{IDA})_3]^{3-}$, (Figure 4). With the extended alkynyl-aryl complexes, the nature of the P substituent (Me vs Ph) does not change the spectral form significantly (Fig. 4 C vs D), although one of the $\Delta J = 2$ transitions around 620 nm is much stronger than in $[\text{Eu}(\text{DPA})_3]^{3-}$.

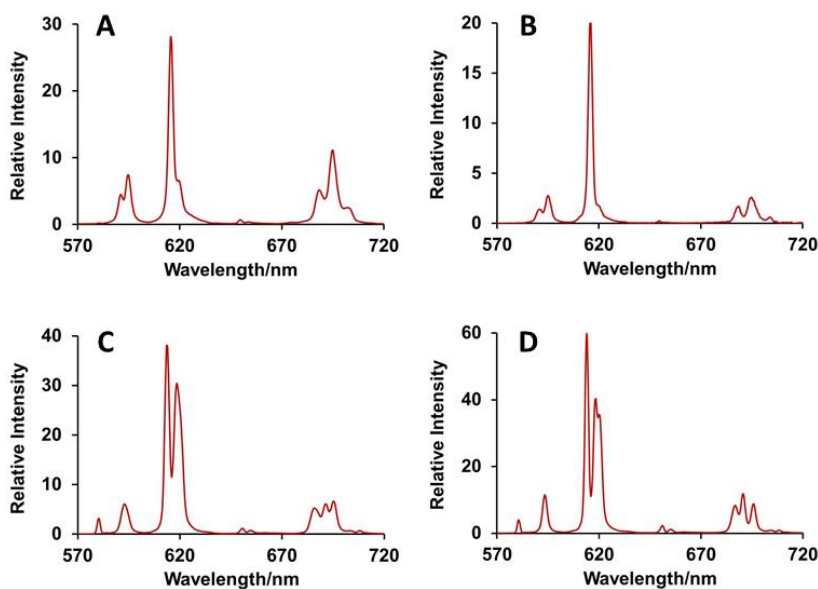


Figure 4. Comparison of total emission spectra for C_3 -symmetric Eu(III) complexes: A) $[\text{Eu}(\text{IDA})_3]^{3-}$ ($\lambda_{\text{exc}} = 395$ nm, H_2O , pH 8.5); B) $[\text{Eu}(\text{DPA})_3]^{3-}$ ($\lambda_{\text{exc}} = 395$ nm H_2O , pH 8.5); C) $[\text{Eu}.\text{L}^{9b}]^{3-}$ ($\lambda_{\text{exc}} = 322$ nm, H_2O , pH 7.4); D) $[\text{Eu}.\text{L}^6]$ ($\lambda_{\text{exc}} = 332$ nm, H_2O , pH 7.4)^{12,23,32}

In europium emission spectra, the oscillator strength of the $\Delta J = 1$ transitions (around 590 nm) is magnetic-dipole (MD) allowed and independent of the ligand environment. In contrast, the $\Delta J = 2$ transitions (around 615 nm) are electric-dipole (ED)-allowed and hypersensitive to ligand perturbation. This behaviour can be rationalised in terms of a ligand polarization model¹⁶ wherein electric-quadrupole-allowed transitions (e.g. $^5\text{D}_0$ to $^7\text{F}_2$) gain significant ED strength via a quadrupole (Ln^{3+})-induced dipole (ligand donor) coupling mechanism. Induced dipoles on the ligands are created by direct coupling to the ED components of the radiation field. Thus, 4f–4f ED strength can be related to ligand dipolar polarisabilities and to the anisotropies of these polarisabilities.¹⁷ Among the ligand donors considered, the polarizable pyridyl groups are common and predominantly define the $\Delta J = 2$ transition oscillator strength. Comparing $[\text{Eu}.\text{L}^1]$ and $[\text{Eu}.\text{L}^3]$, very similar spectra were observed but the $\Delta J = 2/\Delta J = 1$ intensity ratio was 20% higher, consistent with the greater polarisability of the carboxylate over the phosphinate oxygens.

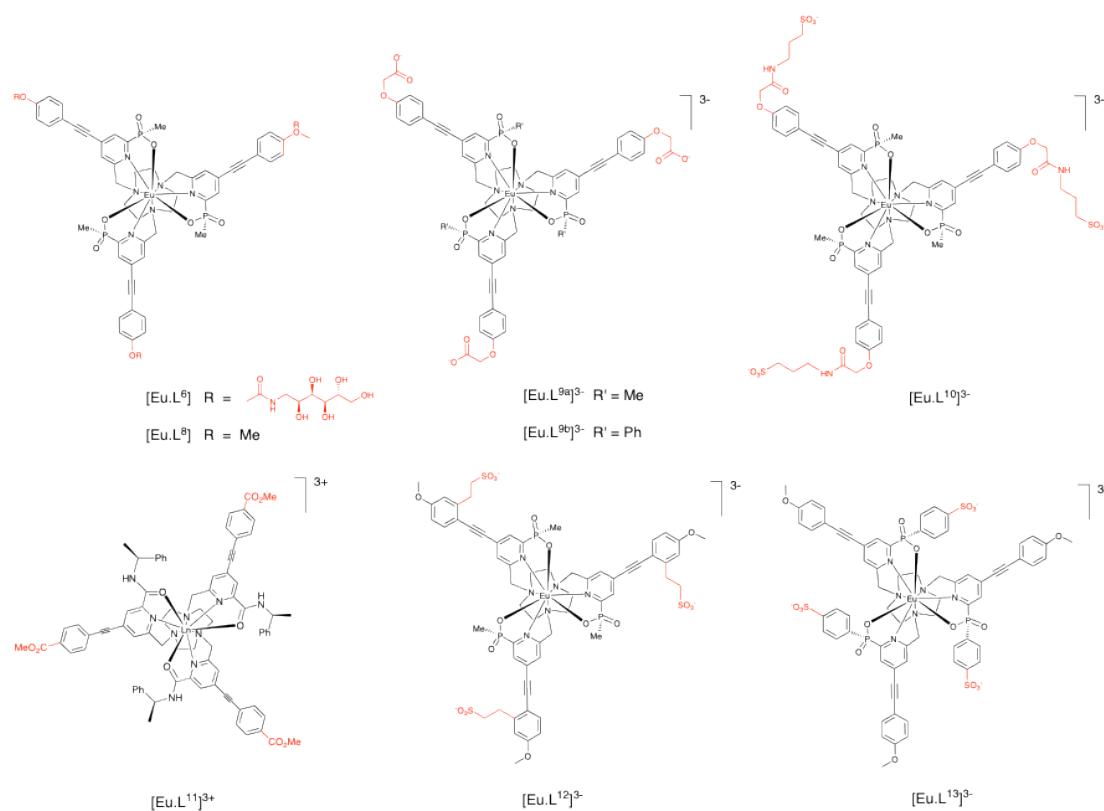


Figure 5 Europium complexes of varying charge and hydrophilicity (Table 1).^{12,21,27,33}

The extinction coefficients of the Eu complexes with extended alkynyl groups lies in the range 55 to $60 \text{ mM}^{-1} \text{ cm}^{-1}$ in water, with lifetimes of around 1 ms and emission quantum yields of 22 to 37% , giving brightness parameters, B , of 12 to $22 \text{ mM}^{-1} \text{ cm}^{-1}$, (Table 1). These are the highest values reported for emissive lanthanide complexes in solution.

Table 1 Selected photophysical and hydrophilicity data for the europium complexes $[\text{EuL}^6]$ and $[\text{EuL}^{8-13}]$ (H_2O , 295 K)^{12,27,33}

Complex	τ/ms	$\epsilon/\text{mM}^{-1} \text{ cm}^{-1}$	$\phi_{\text{em}}/\%$	$\log P^{\text{a}}$
$[\text{Eu.L}^6]$	1.07	56.5	26	n.d.
$[\text{Eu.L}^8]$	1.03	58.1	22	+1.4
$[\text{Eu.L}^{9a}]^{3-}$	1.05	56.6	26	-2.2
$[\text{Eu.L}^{10}]^{3-}$	1.06	56.8	27	-1.5
$[\text{Eu.L}^{11}]^{3+}$	0.80	56.5	37	+0.3
$[\text{Eu.L}^{12}]^{3-}$	1.04	60.1	29	-1.2
$[\text{Eu.L}^{13}]^{3-}$	1.11	58.0	31	+0.7

^a $\log P$ data refer to the distribution of the complex between water and octan-1-ol

Earlier work with tris-dipicolinate complexes possessing arylalkynyl substituents, showed that europium sensitisation involved an intramolecular energy transfer process involving a relaxed and broad ICT excited state, particularly for strongly conjugated electron-donating groups in the aryl group.^{20b} In the case of weaker electron releasing groups, the ICT state lies at higher energy and consequently a contribution from the classical triplet mediated sensitisation process remains possible.^{20a} Variable temperature phosphorescence measurements on the analogous Gd complexes clearly indicated the presence of a triplet excited state at approximately the same energy as the ICT state, (Scheme 2, above). Thus, two sensitisation pathways, namely the triplet state mediated or the direct ICT process could be simultaneously involved in europium sensitisation.²¹ Whatever the mechanism, the Eu complexes show excellent stability with respect to photobleaching, following laser excitation at 355 nm.¹² Such behaviour contrasts with the instability of many organic dyes or of metal complexes bearing sensitisers which have an excited state with $n\pi^*$ character.⁸

These chiral Eu complexes are excellent candidates for study using circularly polarized luminescence (CPL) spectroscopy.^{25-28,31,34,35} The use of CPL spectroscopy allows spectral resolution (Figure 6) of the observed transitions, notably in the $\Delta J = 2$ and 4 manifolds, for the two examples shown here using $[\text{Eu.L}^2]$ and $[\text{Eu.L}^7]$. The very high brightness of $[\text{Eu.L}^7]$ ($B = 33 \text{ mM}^{-1}\text{cm}^{-1}$ in MeOH, 295K) allowed spectral acquisition in a few minutes using a 3 micromolar solution of the complex.³¹ Such enhanced sensitivity with this new range of probes augurs well for the implementation of CPL microscopy, to track the fate of the enantiopure Eu probes and signal any changes in their chiral environment. Proof of principle studies have already demonstrated changes in complex helicity as a result of selective binding to an abundant endogenous chiral anion (e.g. lactate) or a well-defined site in a common protein, e.g. albumin or α_1 -AGP.³⁴⁻³⁸

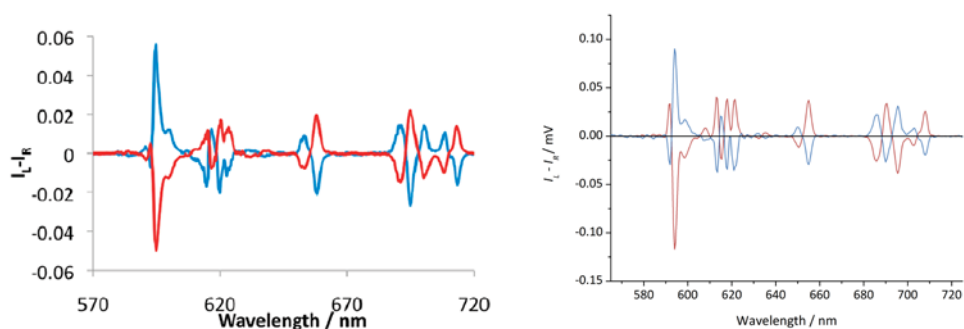


Figure 6 Circularly polarized luminescence spectra for: *left*, Δ - $[\text{Eu.L}^2]$ (blue) and the Λ isomer (red) ($50 \mu\text{M}$, H_2O , 295K, λ_{exc} 280 nm); *right*, Δ (blue) and Λ (red) $[\text{Eu.L}^7]$ ($3 \mu\text{M}$; 295K, MeOH, λ_{exc} 360 nm), showing the enhanced spectral resolution, e.g. for the $\Delta J = 4$ transitions around 700 nm (*viz.* Fig. 4 [C and D] above).^{25,26,31}

Cellular optical imaging

The neutral and cationic Eu complexes (Figure 7) are taken into mammalian cells quite efficiently by macropinocytosis^{12,23}, a process that is promoted by addition of phorbol esters and inhibited by amiloride and wortmannin.³⁹ Macropinocytosis is a form of endocytosis that leads to the formation of leaky macropinosomes of irregular size and shape, the contents of which are readily released into the cytoplasm. This pathway is an attractive means for delivery of the luminescent complexes into the cell, as the complexes can readily escape from the macropinosome, allowing vesicular trafficking to other compartments.

The complexes are well tolerated by a wide variety of primary and transformed cell lines, with IC₅₀ values generally greater than 100 μM. Cell uptake can be quantified by measuring the internalised Eu by ICP-mass spectrometry, and the high brightness means that the concentration of the complex in the incubation medium usually needs to be in the range 500 nM to 20 μM. Uptake in plant cells, roots and pollen tubes has also been examined, with [Eu.L¹⁵] acting as a convenient probe to label the cell walls of plant or root hairs.⁴⁰

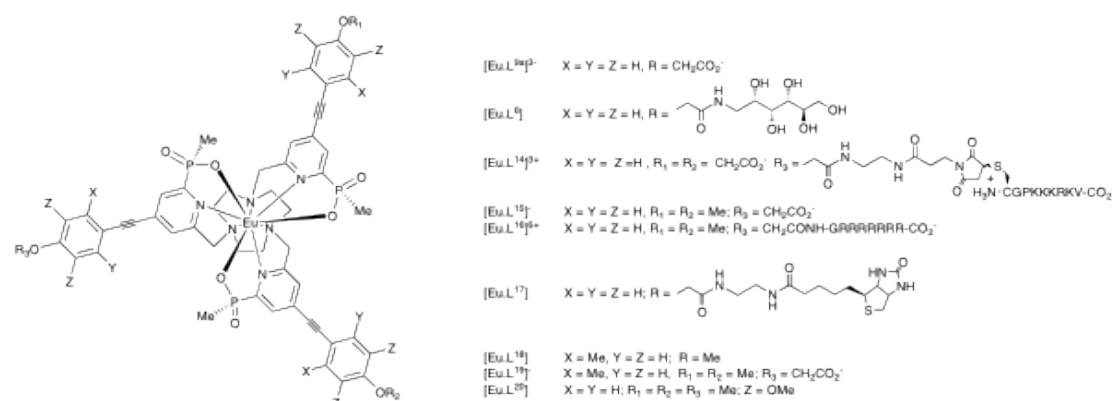


Figure 7 Examples of functionalized Eu complexes, including selected conjugates¹²

The intracellular localization profile of the complexes shown above (Fig. 7) has been studied, and examples of complexes selectively staining the mitochondria (e.g. [Eu.L⁶]), late endosomes and lysosomes (e.g. [Eu.L^{9a13-}]) and the endoplasmic reticulum (e.g. [Eu.L¹⁶³⁺]) were identified. A consequence of the high brightness of the probes is that there is sufficient signal to permit rapid acquisition of both the Eu spectral image and the lifetime of the complex internalized inside the cell. Such studies using time-resolved CCD detection allow the speciation of the Eu complex to be identified; in the majority of cases these reveal the same spectral fingerprint and lifetime to that measured *in vitro*. Such experiments confirm the integrity of the probe when localised inside the cell, (Figure 8) and an absence of change in lifetime confirms resistance to excited state quenching by endogenous electron rich species, such as protein Tyr residues, urate, ascorbate or other reducing agents.⁴¹

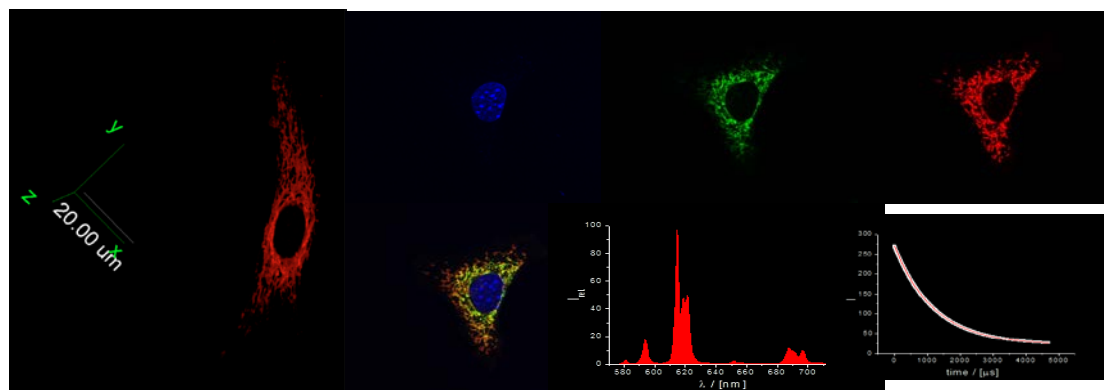


Figure 8 *left*: view of the mitochondrial network of an NIH-3T3 cell stained with the tris-glucamide complex, [Eu.L⁶]; *right*: confocal microscopy images showing: (a) the DAPI stained nucleus (λ_{exc} 355 nm, λ_{em} 400–450 nm); (b) MitoTracker Green staining of the mitochondrial network (λ_{exc} 488 nm, λ_{em} 500–530 nm); (c) mitochondrial localisation of [Eu.L⁷] in NIH 3T3 cells (4h, 30 μM , λ_{exc} 355 nm, λ_{em} 605–720 nm); (d) a merged image showing co-localisation ($P = 0.89$), (e) spectral profiling of [Eu.L⁶] (24h, 30 μM), (f) the intracellular lifetime for [Eu.L⁶] ($\tau_{\text{Eu}} = 1$ ms; 24h, 30 μM).¹²
[ROBERT: CAN YOU MAKE THIS AS GOOD A QUALITY AS POSSIBLE...PLEASE..]

Consideration of Abbé's law, ($d = \lambda/2(n \sin\theta)$, where $n \sin\theta$ is the numerical aperture (NA) = 1.4 here, λ is the excitation wavelength and d is the theoretical resolution) reveals that the use of 488 nm vs 355 nm excitation improves the intrinsic resolution of confocal microscopy from 174 to 126 nm. The images obtained in Figure 8 accord with that view, and the use of a phase modulated resolution enhancement technique allowed microscopic resolution of 65 nm to be achieved.¹² As a result of the high intrinsic brightness of these Eu probes, the power used in pulsed excitation was only 4 mW (<80 nJ/voxel/acquisition). These conditions are very different from those used in the past to examine and quantify UV damage to cells, where continuous light exposure persists for several seconds or minutes and the impact is a steep function of the excitation wavelength. Much less damage occurs above 340 nm.⁴² Indeed, in control experiments examining healthy mouse skin fibroblasts (NIH-3T3 cells) loaded with [Eu.L⁶] (400 nM), following sequential scanning excitation at 355 nm (6 mW) with a 63x objective (NA = 1.4), scanning the same area every 30 minutes for three hours, more than 90% of healthy cells were observed in the field of view. With pulsed excitation at 365 nm (as in Figure 8), even shorter UV exposure times occur.¹²

Examples of responsive probes have also been defined, based on these very bright complexes, in which the Eu spectral fingerprint and lifetime is a sensitive and selective function of local pH or ionic composition.^{30,35,43,44} For example, the reversible intramolecular ligation of the sulphonamide nitrogen in [Eu.L²¹] is a function of pH. This complex localizes well to the endoplasmic reticulum, an organelle that is in equilibrium with the cytosol, so the pH is

equivalent. Careful calibration studies allowed the ratio of two Eu emission bands or the modulation of the emission lifetime to signal pH variation (Figure 9).⁴⁴ Related examples can be imagined, based on reversible anion binding to the Eu centre,⁴³ provided that the probe is able to target the organelle of interest selectively.

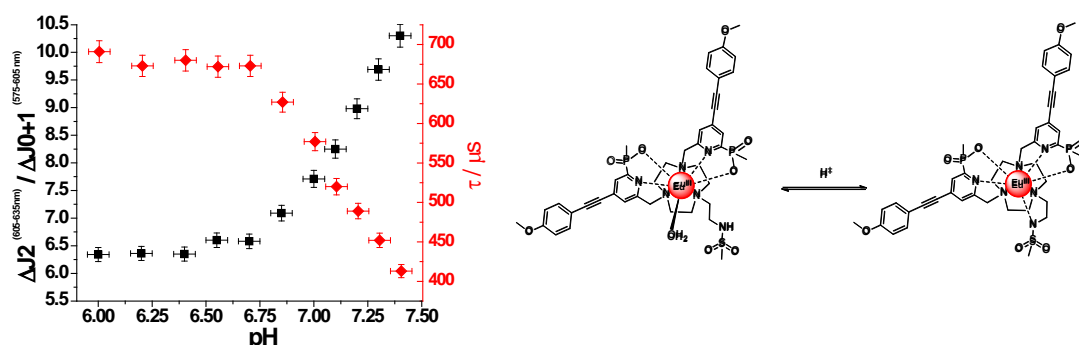


Figure 9 pH variation of the Eu emission intensity ratio ($\Delta J = 2/(\Delta J = 0 + \Delta J = 1)$) and excited state lifetime (τ) for $[\text{Eu.L}^{21}]$ ($\text{pK}_a = 7.15 \pm 0.05$), when the probe is localized in the endoplasmic reticulum of mouse skin fibroblasts (NIH-3T3 cells).⁴⁴

Bioassays based on FRET

The uptake of Eu complexes into cells by macropinocytosis is a disadvantage if you want to develop assays for membrane bound proteins, such as the ubiquitous G-protein coupled receptors.⁴⁵ A non-specific signal is generated due either to the probe sticking at or entering the cell membrane or via binding to immature proteins within the cytosol.^{4a} Bio-conjugates of very water-soluble europium complexes are needed that cannot enter or adhere to cells, at concentrations of less than 1 μM . The cell membrane consists primarily of negatively charged phospholipids, so that several series of 9- N_3 based complexes have been devised that are highly water soluble and negatively charged at physiological pH (Figure 5 above).³³ Any interaction with the cell membrane is suppressed by repulsive electrostatic interactions. Furthermore, the hydrophilic nature of the integral sulphonate and carboxylate groups masks the inherent hydrophobic nature of the three aryl-alkynyl groups, as these are the likely entities that engage in non-specific protein or membrane binding.

In one example, three europium complexes, $[\text{Eu.L}^{22-24}]$ (Figure 10) have been compared, one of which, $[\text{Eu.L}^{22}]$ served as a negative control, as it did not possess peripheral anionic substituents. The complexes were evaluated using 'SNAP-tag' technology on the G-protein coupled receptor, cholecystokinin-2 (CCK-2).⁴⁶ The labeling of the three benzylguanidine-derivatives on living human embryonic kidney cells (HEK293) or HEK293 cells expressing the 'SNAP-tagged' CCK-2 (CCK2-ST) receptor was measured, by monitoring the Eu luminescence at 620 nm. Significant labelling of the unmodified HEK cells occurred with

[Eu.L²²], whereas in the other two cases, non-specific labeling was negligible. Such behaviour paved the way for TR-FRET ligand binding assays using a fluorescent agonist (λ_{em} 665 nm) of the CCK receptor, that serves as an acceptor for the long-lived emission from the Eu donor, both on a plate reader and using TR-FRET microscopy.³³

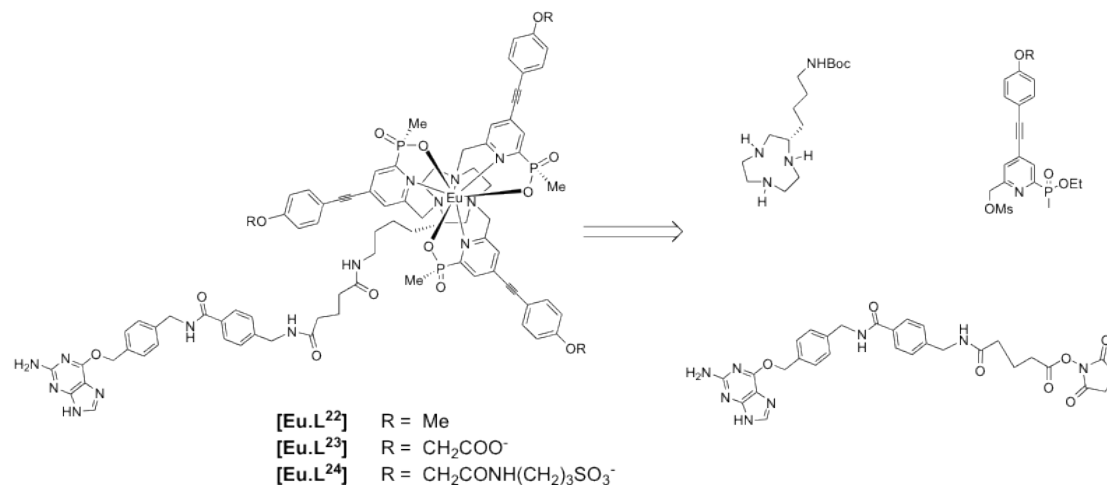


Figure 10 Retrosynthetic strategy to Eu complexes for a ‘SNAP-tagged’ receptor binding assay.³³

[Jurriaan to add a Figure here, as appropriate....colour... and add further comments...please...)

Conclusions and Outlook

The EuroTracker series of emissive complexes based on triazacyclononane possess a brightness that is almost an order of magnitude greater than previously reported Eu(III) systems, and also larger than that of the recombinant red fluorescent protein. The ease of structural manipulation allows close control over the absorption wavelength over the range from 330 to 360 nm and permits various points of attachment to targeting vectors or for biomolecule labeling. The disubstituted series of complexes possess one coordinated water but retain a high quantum yield, and bind anions reversibly. Appropriate substitution of the third ring N should enable the future development of new examples whose emission spectral profile and lifetime can be rendered sensitive to pH, pM and pX, with the required selectivity for the analyte chosen. Enantiopure complexes can be obtained by C-substitution into the 9-membered core ring, aiding the development of chiral probes and tags for the exploration of CPL spectroscopy and microscopy studies.

The series of amphipathic complexes are efficiently taken into many mammalian cells by macropinocytosis, are non-toxic and localise selectively in certain organelles, allowing them to function as selective stains for live-cell imaging studies. By introducing peripheral anionic groups on the rod-like chromophore moieties, non-specific cell uptake is inhibited so that

various conjugates can be devised to aid the development of new organelle-targeted cellular stains and probes or allow new series of bioassays to be undertaken.

Evidently, the future is bright for such rare earth complexes; Sir George Stokes would most probably have approved.

Acknowledgements

This work was supported by the ERC (SJB, ERN, RP, DP; FCC 266804), EC and EPSRC, and is dedicated to the memory of Professor Ken Wade, a friend, colleague and distinguished scientist who understood the meaning of ‘significance’ and ‘originality’.

Notes and references

^a *Department of Chemistry, Durham University, South Road, Durham, DH1 3LE, UK.*

Tel: + 44 (0) 191 33 42033; E-mail: david.parker@dur.ac.uk

1. G. G. Stokes, *Phil. Soc. R. Soc. Lond.* 1852, **142**, 463. Weidemann introduced the term ‘luminescence’ to embrace both short and long-lived temperature independent emission: E. Weidemann, *Ann.der Physik*, 1888, **34**, 446; fluorescence is usually used to describe emission from systems with short-lived, singlet excited states (ns range).
2. K. Przibram, *Nature*, 1935, **135**, 100.
3. J-C. G. Bunzli, *Chem Rev.* 2010, **110**, 2729.
4. a) J. M. Zwieter, H. Bazin, L. Lamarque, G. Mathis, *Inorg. Chem.* 2014, **53**, 1854; b) I. Hemmila and V.-M. Mukkala, *Crit. Rev. Clin. Lab. Sci.*, 2001, **38**, 441.
5. C. P. Montgomery, B. S. Murray, E. J. New, R. Pal, D. Parker, *Acc. Chem. Res.* 2009, **42**, 925.
6. M. C. Heffern, L. M. Matosiuk, T. J. Meade, *Chem. Rev.* 2014, **114**, in press: [dx.doi.org/10.1021/cr400477t](https://doi.org/10.1021/cr400477t).
7. E. G. Moore, A. P. S. Samuel, K. N. Raymond, *Acc. Chem. Res.* 2009, **42**, 542
8. R. A. Poole, C. P. Montgomery, E. J. New, A. Congreve, D. Parker and M. Botta, *Org. Biomol. Chem.* 2007, **5**, 2055; R. A. Poole, G. Bobba, M. J. Cann, J.-C. Frias, D. Parker and R. D. Peacock, *Org. Biomol. Chem.*, 2005, **3**, 1013
9. A.-S. Chauvin, C.D. B. Vandevyver, S. Comby and J.-C. G. Bunzli, *Chem. Commun.*, 2007, 1716; A-S. Chauvin, S. Comby, B. Song, C. D. B. Vandevyver, F. Thomas, J.-C. G. Bunzli, *Chem. Eur-J.*, 2007, **13**, 9515.
10. A. Beeby, I. M. Clarkson, R. S. Dickins, S. Faulkner, D. Parker, L. Royle, A. S. de Sousa, J. A. G. Williams and M. Woods, *J Chem Soc, Perkin Trans 2*, 1999, 493.

11. J. Xu, T. M. Corneille, E. G. Moore, G.-L. Law, N. G. Butlin, K. N. Raymond, *J. Am. Chem. Soc.* 2011, **133**, 19900.
12. S. J. Butler, L. Lamarque, R. Pal and D. Parker, *Chem. Sci.*, 2014, **5**, 1750.
13. (a) P. Chaudhuri, K. Wieghardt, *Progr. Inorg. Chem.* 1987, **35**, 329 (b) E. Cole, R. C. B. Copley, J. A. K. Howard, D. Parker, G. Ferguson, J. F. Gallagher, B. Kaitner, A. Harrison and L. Royle, *J Chem Soc Dalton Trans.*, 1994, 1619;.
14. (a) A. S. Craig, H. Adams, D. Parker and N. A. Bailey, *J Chem Soc Chem Commun* 1989, 1793; (b) C. J. Broan, J. P. L. Cox, A. S. Craig, R. Katakya, D. Parker, A. Harrison, A. M. Randall and G. Ferguson, *J. Chem. Soc. Perkin Trans. 2*, 1991, 87.
15. (a) H. Takalo, I. Hemmila, T. Sutela and M. Latva, *Helv. Chim. Acta* 1996, **79**, 789; (b) C. Gateau, M. Mazzanti, J. Pécaut, F. A. Dunand and L. Helm, *Dalton Trans*, 2003, 2428; (c) G. Nocton, A. Nonat, C. Gateau, and M. Mazzanti, *Helv. Chim. Acta*, 2009, **92**, 2257–2273; (d) J. Hovinen and P. M. Guy, *Bioconjugate Chem.* 2009, **20**, 404; (e) L. Tei, G. Baum, A. J. Blake, D. Fenske and M. Schroder, *Dalton Trans* 2000, 2793; (f) L. Tei, A. J. Blake, C. Wilson and M. Schroder, *Dalton Trans* 2004, 1945.
16. S. F. Mason, R. D. Peacock, B. Stewart, *Mol. Phys.* 1975, **30**, 1829.
17. (a) S. F. Mason, *Struct. Bonding (Berlin)* 1980, **39**, 43; (b) M. F. Reid, F. S. Richardson, *Chem. Phys. Lett.* 1983, **95**, 5012.
18. J. I. Bruce, R. S. Dickins, D. Parker, D. J. Tozer, *Dalton Trans.* 2003, 1264.
19. D. Parker, *Coord. Chem. Rev.*, 2000, **205**, 109.
20. (a) A. Picot, F. Malvolti, B. Le Guennic, P.L. Baldeck, J. A. G. Williams, C. Andraud, O. Maury, *Inorg. Chem.*, **2007**, *46*, 2659; (b) A. D'Aléo, A. Picot, A. Beeby, J. A. G. Williams, B. Le Guennic, C. Andraud, O. Maury *Inorg. Chem.*, **2008**, *47*, 10258; (c) A. Picot, A. D'Aléo, P. L. Baldeck, A. Grichine, A. Duperray, C. Andraud, O. Maury, *J. Am. Chem. Soc.* **2008**, *130*, 1532.
21. M. Soulié, F. Latzko, E. Bourrier, V. Placide, S. J. Butler, R. Pal, J. W. Walton, P. L. Baldeck, B. Le Guennic, C. Andraud, J. M. Zwieter, L. Lamarque, D. Parker and O. Maury, *Chem. Eur. J.*, 2014, **20**, in press.
22. N. C. Shaner, R. E. Campbell, P. A. Steinbach, B. N. G. Giepmans, A. E. Palmer and R. Y. Tsien, *Nature Biotechnology* 2004, **22**, 1567.
23. J. W. Walton, A. Bourdolle, S. J. Butler, M. Soulie, M. Delbianco, B. K. McMahon, R. Pal, H. Puschmann, J. M. Zwieter, L. Lamarque, O. Maury, C. Andraud and D. Parker, *Chem. Commun.*, 2013, **49**, 1600.
24. C. Gateau, M. Mazzanti, J. Pécaut, F.A. Dunand, L. Helm, *Dalton Trans.* 2003, 2428.

25. J. W. Walton, L. Di Bari, D. Parker, G. Pescitelli, H. Puschmann and D. S. Yufit, *Chem Commun*, 2011, **47**, 12289.
26. J. W. Walton, R. Carr, N. H. Evans, A. M. Funk, A. M. Kenwright, D. Parker, D. S. Yufit, M. Botta, S. De Pinto and K. L. Wong, *Inorg Chem*, 2012, **51**, 8042.
27. E. R. Neil, A. M. Funk, D. S. Yufit and D. Parker, *Dalton Trans*. 2014, **43**, 5490.
28. N. H. Evans, R. Carr, M. Delbianco, R. Pal, D. S. Yufit and D. Parker, *Dalton Trans*. 2013, **42**, 15610.
29. J. P. L. Cox, A. S. Craig, I. M. Helps, K.J. Jankowski, D. Parker, M. A. W. Eaton, A. T. Millican, K. Millar, N. R. A. Beeley and B. A. Boyce, *J. Chem. Soc., Perkin Trans.1*, 1990, 2567.
30. S. J. Butler, R. Pal, B. K. McMahon, D. Parker and J. W. Walton *Chem.-Eur. J.* 2013, **19**, 9511.
31. S. J. Butler, M. Delbianco, N. H. Evans, A. T. Frawley, R. Pal, D. Parker, R. S. Puckrin and D. S. Yufit, *Dalton Trans*. 2014, **43**, 5721.
32. J.-G. Kang, T.-J Kim, *Bull. Korean Chem. Soc.* 2005, **26**, 1057.
33. M. Delbianco, V. Sadovnikova, E. Bourrier, L. Lamarque, J. M. Zwier and D. Parker, *Angew. Chem. Int. Ed. Engl.*, 2014, submitted.
34. R. Carr, N. H. Evans and D. Parker, *Chem Soc Rev*, 2012, **41**, 7673.
35. R. Carr, R. Puckrin, B. K. McMahon, R. Pal, D. Parker and L-O. Palsson, *Meth. Adv. Fluoresc.* 2014, in press.
36. C. P. Montgomery, E. J. New, D. Parker, R. D. Peacock, *Chem. Commun.* 2008, 4261.
37. D. M. Dias, J. M. C. Teixeira, I. Kuprov, E. J. New, D. Parker and C. F. G. C. Geraldes, *Org. Biomol. Chem.*, 2011, **9**, 5047.
38. R. Carr, L. Di Bari, S. Lo Piano, D. Parker, R. D. Peacock, J. M. Sanderson, *Dalton Trans*. 2012, **41**, 13154.
39. E. J. New, A. Congreve and D. Parker, *Chem. Sci.*, 2010, **1**, 111.
40. A. J. Palmer, S. H. Ford, S. J. Butler, T. J. Hawkins, P. J. Hussey, R. Pal, J. W. Walton and D. Parker, *RSC Advances*, 2014, **4**, 9356.
41. a) F. Kielar, C. P. Montgomery, E. J. New, D. Parker, R. A. Poole, S. L. Richardson P. A. Stenson, *Org. Biomol. Chem.*, 2007, **5**, 2975; b) G-L. Law, D. Parker, S. L. Richardson and K-L. Wong, *Dalton Trans.*, 2009, 8481.
42. J. C. F. Wong and A. Parisi, 'Assessment of ultraviolet radiation exposures in photobiological experiments', in: Protection Against the Hazards of UVR Internet Conference, 18 Jan - 5 Feb 1999; <http://eprints.usq.edu.au/1279/>.
43. S. J. Butler, and D. Parker, *Chem. Soc. Rev.* 2013, **42**, 1652.
44. B. K. McMahon, R. Pal and D. Parker, *Chem. Commun.* 2013, **49**, 5363.

45. G. Milligan, *Mol. Pharmacol.* 2013, **84**, 158.
46. G. Lukinavičius, K. Umezawa, N. Olivier, A. Honigmann, G. Yang, T. Plass, V. Mueller, L. Reymond, I. R. Corrêa Jr, Z.-G. Luo, C. Schultz, E. A. Lemke, P. Heppenstall, C. Eggeling, S. Manley, K. Johnsson, *Nat. Chem.* **2013**, 5, 132.